

# Effect of Ag addition on crystallization in $\text{As}_2\text{Se}_3$ glasses

M. KITAO, C. GOTOH

*Research Institute of Electronics, Shizuoka University, Hamamatsu 432, Japan*

S. YAMADA

*Department of Electronic Engineering, Shizuoka Institute of Science and Technology, Fukuroi 437, Japan*

Differential scanning calorimetry (DSC) behaviours of glassy  $\text{As}_2\text{Se}_3$  containing Ag up to 5 at % were measured at various heating rates. The effect of addition of Ag on crystallization of glassy  $\text{As}_2\text{Se}_3$  was investigated. The glass transition temperature decreased with increasing Ag content. Crystallization kinetics were analysed on the basis of the two-step process model, where crystal growth takes place after nucleation. For non-doped  $\text{As}_2\text{Se}_3$  two-dimensional growth of crystal was predominant, while for Ag-doped ones three-dimensional growth was very likely. It was supposed for all glassy Ag-doped samples that crystal nuclei exist, though micro-crystallites were not observed on X-ray diffraction traces. The activation energy for crystallization and the glass-forming tendency decreased by the addition of Ag.

## 1. Introduction

In recent years, chalcogenide glass semiconductors have been extensively studied. They are attractive materials because of opto-electronic properties [1]. In order to obtain completely glassy materials, information of crystallization should be required.

Crystallization kinetics of glass-forming materials had been investigated for a long time. The transformation kinetics developed by Johnson and Mehl [2] and Avrami [3] were the earliest works. However, the Johnson–Mehl–Avrami (JMA) model was the rate equation conducted for isothermal conditions. Applications of the JMA model to non-isothermal processes have been discussed by many workers [4,5]. Other analytical methods (for example, the Kissinger-plot [6] and Ozawa-plot [7]) have been proposed for non-isothermal conditions, which are suitable for analysis of differential scanning calorimetry (DSC) results. The limitation of these analytical methods has been pointed out [8]. It is believed generally that glass-forming materials do not crystallize by melt-quenching and become glassy through a supercooled liquid state [8]. In the heating process of DSC measurements, crystallization of glass-forming materials is supposed to take place by a two-step process, where a great number of nuclei generate at a temperature range somewhat higher than the glass transition temperature  $T_g$  and then the crystal growth occurs at much higher temperatures. Considering the two-step process, Matusita *et al.* [9] have proposed the analytical method of DSC curves.

Arsenic triselenide ( $\text{As}_2\text{Se}_3$ ) is a typical chalcogenide glass semiconductor. Glassy  $\text{As}_2\text{Se}_3$  also has a crystal nucleation region just above  $T_g$  and a crystal

growth region at higher temperatures than that. By utilizing the temperature difference between both regions, preparation of  $\text{As}_2\text{Se}_3$  single crystals is possible [10]. Crystallization kinetics of glassy  $\text{As}_2\text{Se}_3$  have been investigated by differential thermal analysis (DTA) [11] and DSC [12]. However, the former was analysed only by Kissinger-plot and the latter was characterized under isothermal conditions. In the Ag–As–Se system, dependence of  $T_g$  on Ag content was reported [13]. Recently, DTA analysis of the Te–As–Se system glasses has been reported in detail [14].

The present paper aims to elucidate the effect of Ag addition on crystallization of glassy  $\text{As}_2\text{Se}_3$  by using DSC. The glass-forming tendency is determined from the glass transition temperature  $T_g$ , the crystallization temperature  $T_c$  and the melting point  $T_m$ . Crystallization kinetics are analysed by the Matusita's non-isothermal method [9], where the crystal growing region is separated from the nucleation region.

## 2. Experimental procedure

Glassy  $\text{As}_2\text{Se}_3$  used was synthesized by heating arsenic and selenium with purities of 99.9999% in an evacuated fused quartz ampoule [15]. The  $\text{As}_2\text{Se}_3$  ingots containing silver as additive ( $\text{As}_{40}\text{Se}_{60}\text{Ag}_x$ ;  $x = 0.5\text{--}5$ ) were prepared by heating the mixture of glassy  $\text{As}_2\text{Se}_3$  and appropriate amounts of Ag (99.999%) in evacuated quartz ampoules under a vacuum of  $10^{-4}$  Pa. The ampoules were placed for 25 h in a rocking furnace whose temperature was kept at about 1000 °C, and then the melts were quenched in air to obtain the glasses. At Ag content of 1 at % or

more, however, a small amount of Ag is often deposited on the surface of the ingot. In order to avoid the deposition of Ag, glassy ingots with  $x \geq 1$  were prepared by the following quenching methods. For Ag contents of 1–1.5 at%, the melts were cooled down to 600 °C in the furnace after synthesis and then quenched in air. For 2–3, 4 and 5 at %, they were quenched in ice-water from 450, 550 and 650 °C, respectively. It was confirmed by X-ray diffraction that the ingots thus obtained are amorphous. It was checked by electron probe X-ray microanalysis (EPMA) that Ag atoms are distributed uniformly over the ingots, and that the chemical composition of ingots is equal to the ratio of weighted raw materials.

Measurements of DSC were carried out by using a SSC5200 thermal analyser with a DSC220 differential scanning calorimeter. Typically, 8 mg of sample in granular form (grain size was more than 0.1 mm) was sealed in standard aluminium pans. The same type of pan containing 10 mg of  $\alpha$ -alumina was employed as the reference cell. Before the DSC measurements, samples were annealed at 120 °C for 1 h in the DSC apparatus in order to stabilize the glass structure and eliminate the effect of thermal history. DSC measurements were performed from 30 to 480 °C using uniform heating rates of 1–20 K min<sup>-1</sup>.

### 3. Experimental results

DSC measurements of glassy As<sub>40</sub>Se<sub>60</sub>Ag<sub>x</sub> were carried out for different heating rates. DSC thermograms

at 5 K min<sup>-1</sup> for samples with various  $x$  are shown in Fig. 1a ( $x = 0, 0.5, 1$  and 1.5) and Fig. 1b ( $x = 2, 3, 4$  and 5). As seen in the figures, the glass transition temperature  $T_g$  and the melting point  $T_m$  decrease with increasing Ag content. On the other hand, the crystallization temperature  $T_c$ , which is defined as the peak temperature of exotherm curve, is not dependent monotonically on the Ag content because of complicated exotherm curves. Behaviours of  $T_g$ ,  $T_m$  and  $T_c$  for other heating rates are similar to those described above.

Fig. 2 shows DSC thermograms of glassy As<sub>40</sub>Se<sub>60</sub>Ag<sub>3</sub> for different heating rates.  $T_g$  and  $T_c$  shifts to high temperatures with increasing heating rate, while  $T_m$  is independent of the heating rate. For the samples with other Ag contents, the same results are obtained.

### 4. Discussion

Glass-forming region of As<sub>40</sub>Se<sub>60</sub>Ag<sub>x</sub> was reported to range up to about 10 at % of silver [16]. Above 1 at % of Ag, however, glass formation does not easily occur and Ag atoms often deposit on the surface. In order to examine the glass-forming tendency of As<sub>40</sub>Se<sub>60</sub>Ag<sub>x</sub>, the glass-forming ability  $K_{gl}$  [17]

$$K_{gl} = (T_c - T_g)/(T_m - T_c) \quad (1)$$

was calculated. The results at heating rate of 5 K min<sup>-1</sup> are tabulated in Table I. If  $K_{gl} \geq 0.1$ , the preparation of glass was pointed out to become easy

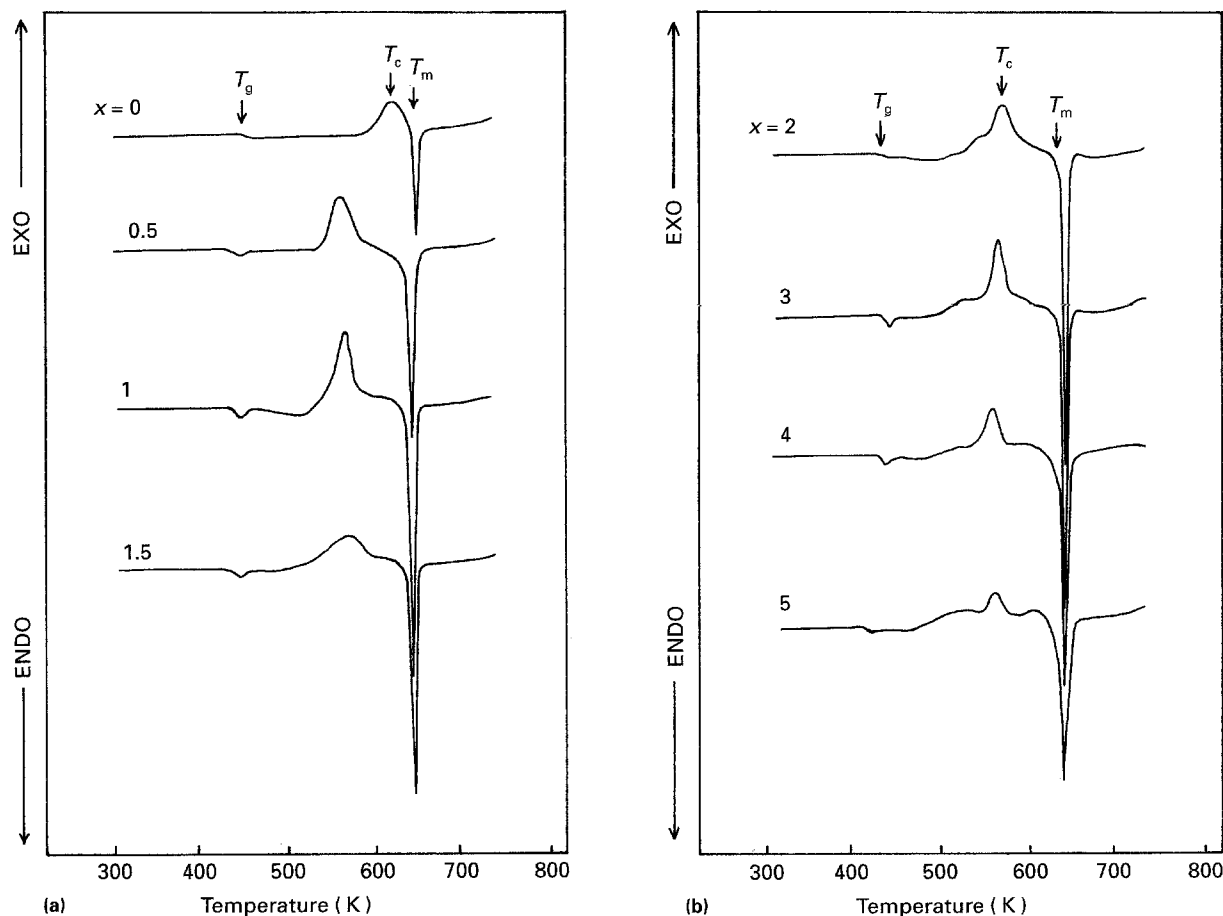


Figure 1 DSC traces for glassy As<sub>40</sub>Se<sub>60</sub>Ag<sub>x</sub> at a heating rate of 5 K min<sup>-1</sup>. (a)  $x = 0$ –1.5, (b)  $x = 2$ –5.

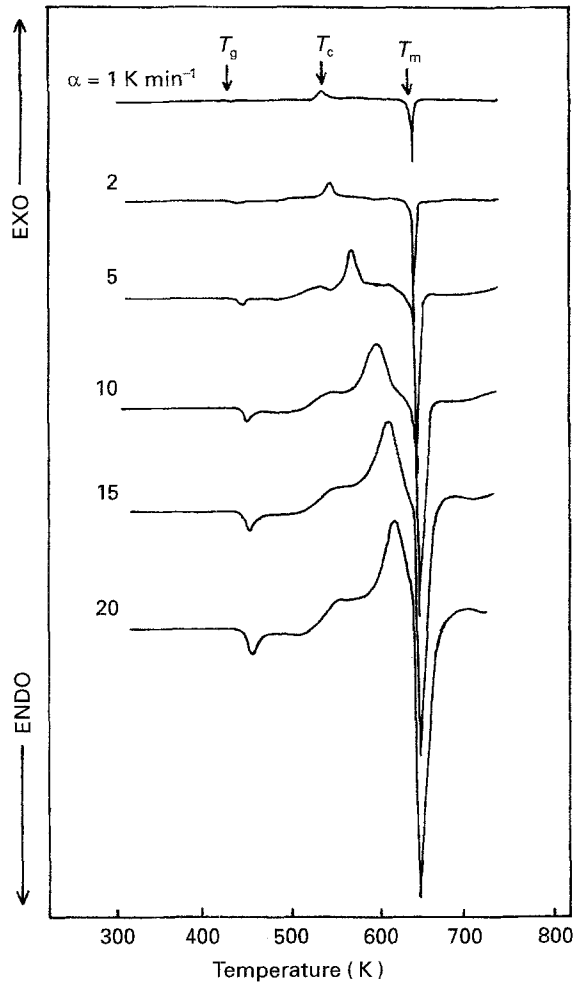


Figure 2 DSC traces for glassy  $\text{As}_{40}\text{Se}_{60}\text{Ag}_3$  at various heating rates.

TABLE I The glass-forming ability  $K_{gl}$  for glassy  $\text{As}_{40}\text{Se}_{60}\text{Ag}_x$

$x$	$K_{gl}$
0	9.5
0.5	1.7
1	1.8
1.5	2.0
2	2.1
3	2.1
4	1.7
5	1.6

[17]. By the addition of Ag,  $K_{gl}$  decreases abruptly to be about one-fifth of the non-doped sample. However, all of the samples are satisfied with the condition that  $K_{gl} \geq 0.1$ . They are noticed to be good glass formers.

Crystallization of glass-forming materials is considered to go through the two-step process, where crystal nucleation is motivated at temperatures somewhat higher than  $T_g$  and then crystal growth begins at temperatures higher than those. When the sample is heated at a constant rate  $\alpha$ , a great number of nuclei form firstly. If the crystals grow in  $m$ -dimensions from the nuclei, the variation of crystal volume fraction  $y$  is given by the following equation [9]

$$dy/dt = A_1(1-y) \alpha^{-(n-1)} \exp\left(-\frac{mE}{kT}\right) \quad (2)$$

where  $E$  is the activation energy for crystallization,  $k$  the Boltzmann constant,  $A_1$  a constant and  $m$  the dimension of crystal growth.  $n$  is the numerical factor, value of which is  $m+1$  and  $m$  for the starting samples containing no nucleus and a large number of nuclei, respectively [9].

Integrating Equation 2 and then taking the logarithm of the resulting expression leads to the following equation

$$\ln[-\ln(1-y)] = A_2 - n \ln \alpha - \frac{mE}{kT} \quad (3)$$

This equation represents the relation between the crystal volume fraction  $y$  and the activation energy  $E$  at non-isothermal process. Here,  $y$  was obtained as a function of temperature from the area under DSC exotherm curve due to crystallization [18].

For a certain temperature, Equation 3 can be written in the form

$$\ln[-\ln(1-y)] = -n \ln \alpha + \text{constant} \quad (4)$$

Plots of  $\ln[-\ln(1-y)]$  versus  $\ln \alpha$  for different temperatures yield straight lines, whose slope gives a value of  $n$ . Fig. 3 shows the plots for (a) non-doped  $\text{As}_2\text{Se}_3$  and (b)  $\text{As}_{40}\text{Se}_{60}\text{Ag}_2$ .

For a uniform heating rate, Equation 3 becomes

$$\ln[-\ln(1-y)] = -\frac{mE}{kT} + \text{constant} \quad (5)$$

Fig. 4 shows the relation between  $\ln[-\ln(1-y)]$  and  $1/T$  for (a)  $\text{As}_2\text{Se}_3$  and (b)  $\text{As}_{40}\text{Se}_{60}\text{Ag}_2$ . At high temperatures, a change in slope is seen for all the heating rates. In all the samples with other Ag contents, a similar change to that shown in Fig. 4 for all the heating rates is observed also. It was pointed out [19] that the break in slope is attributed to the saturation of nucleation sites in the final stages of crystallization and/or to restriction of crystal growth by the contact of the crystalline particles. Accordingly, values of  $mE$  for various  $\alpha$  are determined from slopes of linear portion at lower temperatures.

When the crystal volume fraction  $y$  is fixed, the relation between  $\alpha$  and  $T$  is derived from Equation 3 as follows

$$\ln \alpha = (-mE/n)(kT)^{-1} + \text{constant} \quad (6)$$

From the slope of  $\ln \alpha$  against  $1/T$  (see Fig. 5), values of  $mE/n$  are calculated for  $y = 0.3$  and  $0.5$ .

The average values of  $n$ ,  $mE$  and  $mE/n$  thus obtained are tabulated in Table II. From these values in the table, the values of crystallization parameters ( $m$ ,  $n$  and  $E$ ) cannot be strictly determined. As the starting samples were checked to be amorphous by X-ray diffraction, value of  $m$  may be assumed to be equal to  $n-1$ . If so,  $m = 1$  in samples with Ag content of 1.5 and 2 at %. This suggests that growth is one-dimensional. We confirmed experimentally that one-dimensional growth ( $m = 1$ ) was always derived from the same kind of analytic calculations whenever powdered samples (grain size of 0.01 mm or less) were employed in DSC measurements. In this case, surface crystallization is considered to be predominant. In

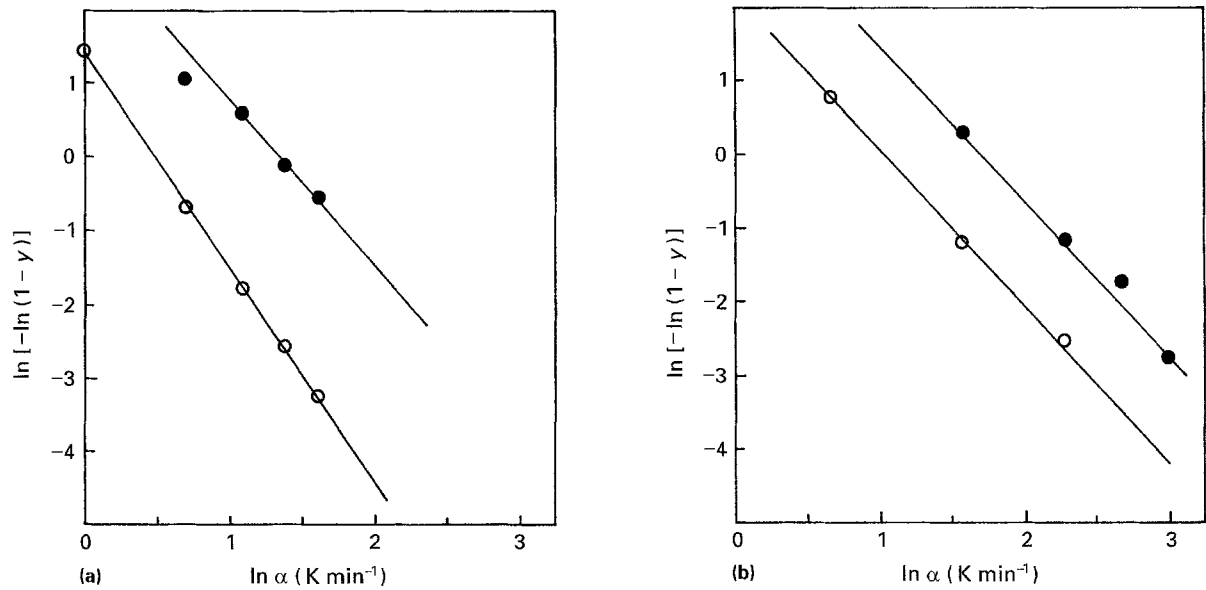


Figure 3 Variation of  $\ln [-\ln(1-y)]$  against  $\ln \alpha$  for (a)  $\text{As}_2\text{Se}_3$  ( $\circ$   $I = 603 \text{ K}$ ;  $\bullet$   $I = 623 \text{ K}$ ) and (b)  $\text{As}_{40}\text{Se}_{60}\text{Ag}_2$  ( $\circ$   $I = 563 \text{ K}$ ;  $\bullet$   $T = 583 \text{ K}$ ). From the slope of the straight line,  $n$  is determined, (a)  $\bullet$  2.3,  $\circ$  3.0; (b)  $\bullet$  2.0,  $\circ$  2.1.

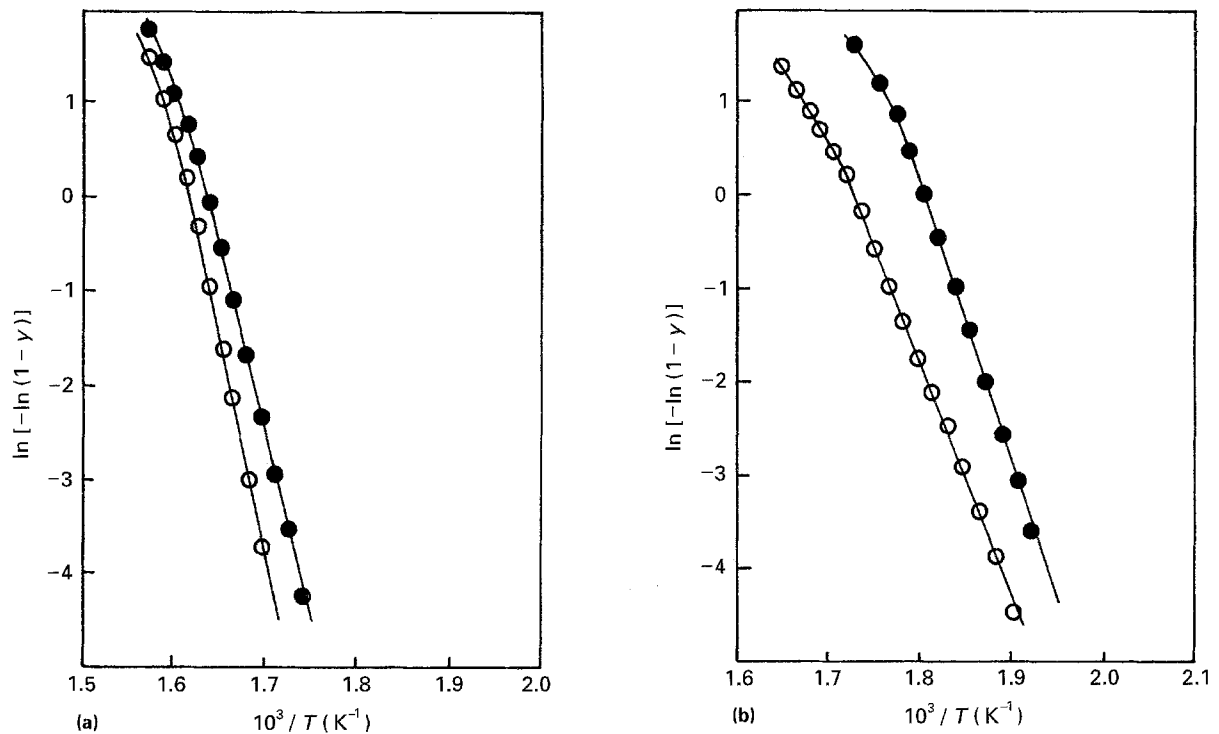


Figure 4 Variation of  $\ln [-\ln(1-y)]$  against reciprocal temperature for (a)  $\text{As}_2\text{Se}_3$  and (b)  $\text{As}_{40}\text{Se}_{60}\text{Ag}_2$ . From the slope at low temperatures,  $mE$  is determined. (a)  $\bullet$   $\alpha = 2 \text{ K min}^{-1}$ ,  $mE = 3.6 \text{ eV}$ ;  $\circ$   $\alpha = 3 \text{ K min}^{-1}$ ,  $mE = 4.1 \text{ eV}$ . (b)  $\bullet$   $\alpha = 2 \text{ K min}^{-1}$ ,  $mE = 2.5 \text{ eV}$ ;  $\circ$   $\alpha = 5 \text{ K min}^{-1}$ ,  $mE = 2.1 \text{ eV}$ .

glassy  $\text{As}_{40}\text{Se}_{60}\text{Ag}_x$  ( $x = 1.5$  and  $2$ ) sample, however, the one-dimensional crystal growth is believed not to be suitable for the actual circumstances. DSC exotherm traces of the samples with around 2 at % Ag do not give simple shapes of crystallization peaks as shown in Fig. 1. It is then supposed that the calculation errors come about in the above analysis.

In order to determine the crystallization parameters, the activation energy  $E$  for crystallization is evaluated separately from Kissinger's formula [6]

$$\frac{E\alpha}{kT_c^2} = A \exp\left(-\frac{E}{kT_c}\right) \quad (7)$$

where  $T_c$  is the crystallization temperature, at which the rate of increase of crystal volume fraction  $y$  is a maximum. The equation obtained by differentiating Equation 2,  $d(dy/dt)/dt$ , is similar to Equation 7. By using the activation energy obtained from Equation 7, therefore, it is considered that the values of other crystallization parameters are also determined. Fig. 6 shows the relation between  $\ln(\alpha/kT_c^2)$  and  $1/T_c$  (Kissinger-plot) for samples with various Ag contents. The activation energies are obtained from the slope in the Kissinger-plot. Now if modes of dimension of crystal growth are not mixed on simplicity, we can assume that the dimension of crystal growth ( $m$ -value)

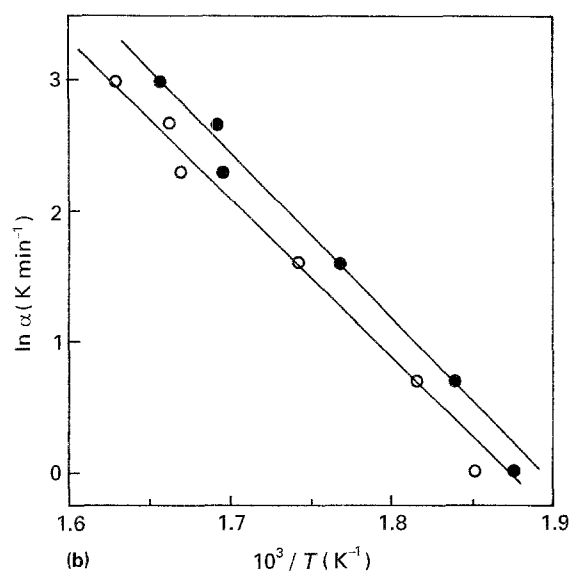
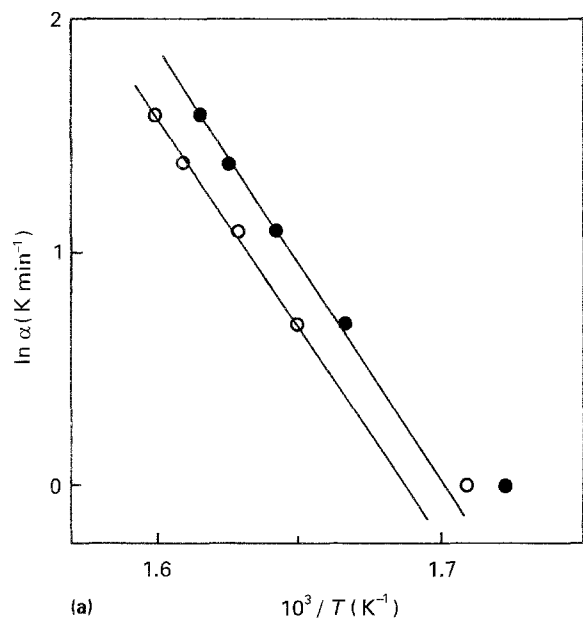


Figure 5 Variation of  $\ln \alpha$  against reciprocal temperature at  $y = 0.3$  (●) and  $0.5$  (○) for  $\text{As}_2\text{Se}_3$  and (b)  $\text{As}_{40}\text{Se}_{60}\text{Ag}_2$ . From the slope of the straight line,  $mE/n$  is determined, (a) 1.6 eV, (b) 1.1 eV.

TABLE II Values of parameters ( $n$ ,  $mE$  and  $mE/n$ ) calculated from DSC data for glassy  $\text{As}_{40}\text{Se}_{60}\text{Ag}_x$

$x$	$n$	$mE$ (eV)	$mE/n$ (eV)
0	2.7	3.9	1.6
0.5	3.3	3.5	1.2
1	2.7	2.7	1.1
1.5	1.8	2.0	1.0
2	2.0	2.3	1.1
3	3.0	2.8	0.9
4	3.5	4.7	1.3
5	3.2	4.8	1.4

is an integer. Then values of crystallization parameters evaluated from results in Table II and the Kissinger-plot are listed in Table III.

In non-doped  $\text{As}_2\text{Se}_3$ ,  $m = 2$  as shown in Table III. Single crystal of  $\text{As}_2\text{Se}_3$  has a layered structure belonging to the monoclinic system [10]. Accordingly, two-dimensional growth is reasonable to be dominant

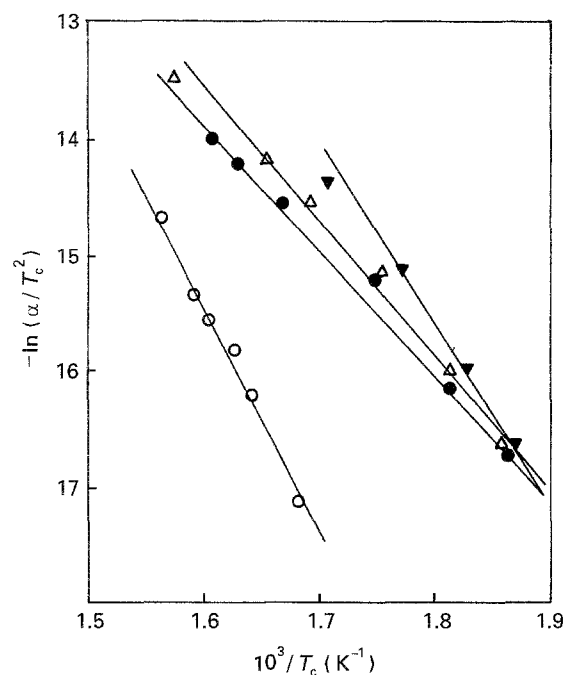


Figure 6 Kissinger-plot of data obtained from DSC curves for  $\text{As}_{40}\text{Se}_{60}\text{Ag}_x$ .  $T_c$  is the crystallization temperature, which is peak temperature of DSC exotherm curve. From the slope of straight line, the activation energy for crystallization is determined.  $x = 0$  (○), 1 (△), 3 (●), 5 (▼).

TABLE III Values of the activation energy ( $E$ ), the dimension of growth ( $m$ ; integer) and the numerical factor ( $n$ ; integer) depending on crystallization mechanism for glassy  $\text{As}_{40}\text{Se}_{60}\text{Ag}_x$

$x$	$E$ (eV)	$m$	$n$
0	1.7	2	3
0.5	1.0	3	3
1	1.0	3	3
1.5	1.0	2	2
2	1.1	2	2
3	1.0	3	3
4	1.3	3	3
5	1.4	3	3

in  $\text{As}_2\text{Se}_3$ . In samples with Ag content of 0.5 and 1 at %,  $m = 3$ . If added Ag atoms are situated between layers of  $\text{As}_2\text{Se}_3$ , three-dimensional crystal growth is considered to be plausible. In a similar phenomenon, Mn atoms were suggested to be situated at interlayer positions from the measurements of electron spin resonance (ESR) [20] and a.c. conductivity [21]. For 1.5–2 at % Ag,  $m = 2$  again. The density of Mn atoms situated at interlayer positions were pointed out to saturate above 0.1 at % [20]. As the Ag content increases, the density of Ag situated between layers may saturate. If so, Ag atoms above 1 at % are considered to tend to bond with As or Se atoms within each layer, so that two-dimensional growth is likely. When Ag content is 3 at % or more, samples may be regarded as the Ag–As–Se ternary system. The compound  $\text{AgAsSe}_2$  has an orthorhombic or tetragonal structure [22]. In such a high content region of Ag, therefore, three-dimensional growth should be brought about.

As seen in Table III,  $n = m + 1$  for non-doped  $\text{As}_2\text{Se}_3$  and, on the other hand,  $n = m$  for all the Ag-doped ones. From these facts, accordingly, it is

interpreted that the starting pure  $\text{As}_2\text{Se}_3$  samples have no nuclei, while the samples of  $\text{As}_2\text{Se}_3$  with Ag may contain a large number of nuclei. Since the temperature range of crystal growth is higher than that of nucleation, the particles are considered not to grow up to the limit of detectability of crystallinity by X-ray diffraction. Even though nuclei exist, therefore,  $\text{As}_2\text{Se}_3$  with Ag additive is still glassy.

The activation energy for crystallization can be interpreted to correspond to the energy barrier of transformation from the glassy to crystalline phase. As shown in Table III, the activation energy decreases abruptly by the addition of Ag. The activation energy of  $\text{As}_{40}\text{Se}_{60}\text{Ag}_x$  ( $x \neq 0$ ) is constant irrespective of Ag content, but it increases a little in the Ag content region of 4–5 at %. The dependence of the activation energy on Ag content up to 3 at % Ag corresponds to that of the glass-forming ability (see Table I). It is understood, therefore, that the addition of Ag into glassy  $\text{As}_2\text{Se}_3$  induces crystallization to stimulate. At the Ag content of more than 3 at %, however, a little different result is obtained, because  $\text{As}_2\text{Se}_3$  with high content of Ag is considered to form a few kinds of crystal structures ( $\text{AgAsSe}_2$ ,  $\text{Ag}_3\text{AsSe}_3$ , etc.) in the Ag–As–Se system.

## 5. Conclusions

From the thermal analysis of glassy  $\text{As}_2\text{Se}_3$  with Ag content up to 5 at % by DSC measurements, the following results and conclusions about crystallization have been obtained.

1. The glass transition temperature decreases with increasing Ag content.

2. Although the glass-forming ability decreases by the addition of Ag, all the samples are good glass-forming materials.

3. In non-doped  $\text{As}_2\text{Se}_3$ , two-dimensional crystal growth is predominant. In Ag-doped ones, on the other hand, it changes to three-dimensional growth. However, it turns again to two-dimensional growth at Ag content of around 2 at %.

4.  $\text{As}_2\text{Se}_3$  containing Ag has nuclei even in as-quenched samples. However, the existence of crystalline particles could not be detected by X-ray diffraction.

5. Dependence of the activation energy for crystallization on the Ag content shows a similar behaviour to that of the glass-forming ability.

The preparation of glassy  $\text{As}_2\text{Se}_3$  containing Ag up to 5 at % is found to be possible. Because of the

existence of crystal nuclei and the decrease of glass-forming tendency due to Ag addition, however, attention should be paid sufficiently to the cooling process for the preparation of completely glassy samples.

## Acknowledgement

The authors would like to express their sincere thanks to Mr K. Urabe for technical assistance of sample preparation.

## References

1. S. R. ELLIOTT, "Glasses and amorphous materials", Vol. 9 edited by J. Zarzycki (Materials Science and Technology, VCH, Weinheim, 1991) p. 375.
2. W. A. JOHNSON and K. F. MEHL, *Trans. Am. Inst. Mining Met. Engrs* **135** (1939) 416.
3. M. AVRAMI, *J. Chem. Phys.* **7** (1939) 1103.
4. S. SURINACH, M. D. BARO, M. T. CLAVAGUERA-MORA and N. CLAVAGUERA, *J. Non-Cryst. Solids* **58** (1983) 209.
5. R. A. LIGERO, J. VAZQUEZ, P. VILLARES and R. JIMENZ-GARAY, *Mater. Lett.* **8** (1989) 6.
6. H. E. KISSINGER, *Anal. Chem.* **29** (1957) 1702.
7. T. OZAWA, *J. Thermal Anal.* **2** (1970) 301.
8. H. YINNON and D. P. UHLMANN, *J. Non-Cryst. Solids* **54** (1983) 253.
9. K. MATUSITA, T. KOMATSU and R. YOKOTA, *J. Mater. Sci.* **19** (1984) 291.
10. M. KITAO, N. ASAKURA and S. YAMADA, *Jpn J. Appl. Phys.* **8** (1969) 499.
11. D. D. THORNBURG and R. I. JOHNSON, *J. Non-Cryst. Solids* **17** (1975) 2.
12. D. W. HENDERSON and N. J. AST, *ibid.* **64** (1984) 43.
13. P. PATEL and N. J. KREIDL, *J. Amer. Ceram. Soc.* **58** (1975) 263.
14. M. K. KOTKATA, M. H. EL-FOULY and S. A. FAYEK, *J. Mater. Sci.* **25** (1990) 2917.
15. M. KITAO, *Jpn J. Appl. Phys.* **11** (1972) 1472.
16. Z. U. BORISOVA and T. S. RYKOVA, *Sov. J. Phys. Chem. Glasses* **3** (1977) 537.
17. A. HRUBY, *Czech. J. Phys. B* **22** (1972) 1187.
18. K. MATUSITA and S. SAKKA, *Phys. Chem. Glasses* **20** (1979) 81.
19. S. MAHADEVAN, A. GIRIDHAR and A. K. SINGH, *J. Non-Cryst. Solids* **88** (1986) 11.
20. I. WATANABE, Y. INAGAKI and T. SHIMIZU, *ibid.* **22** (1976) 109.
21. Y. TAKANO, M. KITAO and S. YAMADA, *Philos. Mag. B* **55** (1987) 515.
22. YU. V. VOROSHILOV, M. I. GOLOVEI and M. V. POTORII, *Sov. Phys. Crystallog.* **21** (1976) 333.

Received 15 December 1993  
and accepted 3 February 1995